Received June 4, 2019, accepted June 17, 2019, date of publication June 20, 2019, date of current version July 3, 2019.

Digital Object Identifier 10.1109/ACCESS.2019.2923905

Ensemble Approach of Optimized Artificial Neural Networks for Solar Photovoltaic Power Prediction

SAMEER AL-DAHIDI[1], OSAMA AYADI[2], MOHAMMED ALRBAI[2], AND JIHAD ADEEB[2,3]

[1]Department of Mechanical and Maintenance Engineering, School of Applied Technical Sciences, German Jordanian University, Amman 11180, Jordan
[2]Mechanical Engineering Department, The University of Jordan, Amman 11942, Jordan
[3]Renewable Energy Center, Applied Science Private University, Amman 11931, Jordan

Corresponding author: Sameer Al-Dahidi (sameer.aldahidi@gju.edu.jo)

ABSTRACT The use of data-driven ensemble approaches for the prediction of the solar Photovoltaic (PV) power production is promising due to their capability of handling the intermittent nature of the solar energy source. In this work, a comprehensive ensemble approach composed by optimized and diversified Artificial Neural Networks (ANNs) is proposed for improving the 24h-ahead solar PV power production predictions. The ANNs are optimized in terms of number of hidden neurons and diversified in terms of the diverse training datasets used to build the ANNs, by resorting to trial-and-error procedure and BAGGING techniques, respectively. In addition, the Bootstrap technique is embedded to the ensemble for quantifying the sources of uncertainty that affect the ensemble models' predictions in the form of Prediction Intervals (PIs). The effectiveness of the proposed ensemble approach is demonstrated by a real case study regarding a grid-connected solar PV system (231 kWac capacity) installed on the rooftop of the Faculty of Engineering at the Applied Science Private University (ASU), Amman, Jordan. The results show that the proposed approach outperforms three benchmark models, including smart persistence model and single optimized ANN model currently adopted by the PV system's owner for the prediction task, with a performance gain reaches up to 11%, 12%, and 9%, for *RMSE*, *MAE*, and *WMAE* standard performance metrics, respectively. Simultaneously, the proposed approach has shown superior in quantifying the uncertainty affecting the power predictions, by establishing slightly wider PIs that achieve the highest confidence level reaches up to 84% for a predefined confidence level of 80% compared to three other approaches of literature. These enhancements would, indeed, allow balancing power supplies and demands across centralized grid networks through economic dispatch decisions between the energy sources that contribute to the energy mix.

INDEX TERMS Artificial neural networks, ensemble, photovoltaic power, prediction, bootstrap, uncertainty quantification.

I. INTRODUCTION

The contribution of Renewable Energy (RE) sources to the energy production portfolio is boosting compared to other available productions obtained by alternative conventional energy sources, such as natural gas, oil, and coal [1]–[6]. The global RE production capacity raised by 171 GW (growth by 7.9% during 2018) reaching 2,351 GW worldwide, at the end of 2018 [5], [7]. The solar power produced by Photovoltaic (PV) accounted for 20% (486 GW) of the total global RE production at the end of 2018, with a capacity increase of 94 GW (+24%) [8], [9]. Due to the significant cost reductions of solar energy productions, solar PV modules, and the competitive procurement of solar PV systems, this source of energy starts to have a potential rule in the global energy production [10]. For example, the Levelised Cost Of Electricity (LCOE) of solar PV has been decreased (and it continues to show a decreasing trend) by 73% between 2010 and 2017, while the energy conversion efficiency has been improved [11], [12].

The effective contribution of solar PV production to the energy mix requires the availability of prediction (forecasting) models capable of providing accurate power production predictions [13]–[15]. For instance, for solar PV systems, electricity traders are interested in finding means for having accurate short-term prediction (e.g., one-day ahead) of production from such systems [16]. In practice, having the capability of accurately predicting the solar PV production

The associate editor coordinating the review of this manuscript and approving it for publication was Natarajan Prabaharan.

for, e.g., one-day ahead, has, indeed, several economic benefits, including reliable operation planning, scheduling of generation, efficient electricity market operations, and proactive power trading [15], [17]. However, production prediction from such energy sources depends on intermittent (stochastic) weather variables, such as solar radiation, wind speed, and ambient temperature, which lead to large uncertainties in solar power production predictions [18]–[22].

Generally, the prediction approaches can be categorized into model-based and data-driven [23]–[26]. The former approaches rely on physics-based models that use weather variables for solar PV power production predictions. However, the adopted models entail making assumptions and simplifications, which constitutes difficulties for their practical deployment. On the contrary, data-driven approaches, which are usually developed by resorting to the so-called machine learning techniques, completely rely on the available pairs of historical actual or forecasted weather data and the associated power production, collected during the operation of the PV plant, with no need to employ any explicit physics-based models.

Several data-driven methods were proposed and applied to solar PV power production prediction, e.g., Artificial Neural Networks (ANNs) [27], Gradient Boosting Regression Trees (GBRT) [28], Support Vector Machines (SVMs) [29], and Extreme Learning Machines (ELMs) [25]. However, there is no unique method capable of accurately predicting the solar PV power production. In fact, the application of different data-driven methods using the same weather/power data, or the same method with different internal parameter settings can lead to different predictions accuracies [30].

To overcome this challenge, ensemble approaches, which aggregate the predictions provided by multiple prediction models (hereafter called base models), are developed and showed to be a better mean in boosting the predictions accuracy, with respect to any sole model of the ensemble, and at the same time quantifying their associated uncertainty [31], [32]. For example, Omar *et al.* [33], developed ensembles of multilayer perceptron feedforward ANNs models that receive the weather forecasts of the next day as an input and produce more generalized one day-ahead production predictions as an output of a solar facility; Pierro *et al.* [34], developed an outperforming Multi-Model Ensemble (MME) that averages the 24h-ahead solar PV power production obtained by the best different data-driven base models fed with different numerical weather prediction input data.

Independently from the adopted prediction model and of the scheme implemented to provide the final power predictions (i.e., individual model or ensemble of prediction models), various sources of uncertainty might affect the predictions, leading to non-accurate, possibly misleading, information for grid operation [35].

In this context, the objective of this work is to develop a new comprehensive ensemble approach composed by several ANNs base models for *i)* 24h-ahead predicting the solar PV power production, as accurate as possible, and then, *ii)* quantifying the associated uncertainty. The ANN base model is optimized in terms of number of hidden neurons, H, to further enhance the prediction accuracy. The motivation behind the choice of ANNs is due to their simplicity, capability of solving non-linear interpolation problems, and the easiness of their implementations [36], [37].

The proposed approach requires: *1)* generating multiple diverse base prediction models, and *2)* aggregating their predictions by a given strategy of aggregation.

With respect to 1), it is shown that the more diversified base prediction models are, the better prediction accuracy of the ensemble outcome can be obtained [38]–[40]. Several methods were proposed in literature to achieve diversity among the ensemble models, like adopting different types of prediction models, adopting the same prediction model type but with different parameter settings, or building/training each prediction model with different training datasets, by resorting to techniques such as Bootstrapping AGGregatING (BAGGING) [40], [41], Boosting [42], and Adaboost [43]. In this work, BAGGING technique (which is based on training the multiple base models using different training sets, whose training patterns are sampled randomly with replacement from the original available training dataset) is employed since it is shown capable of enhancing the prediction performance and it is easy to implement [41], [44].

With respect to 2), once the base prediction models of the ensemble are developed, an effective strategy for aggregating their prediction outcomes is required. Aggregation strategies can be generally categorized into statistics-based and model performance-based [39], [45], [46]. The former strategies assume that the base models contribute equally to the final prediction outcome of the ensemble by simply computing statistical values, e.g., average or median, of the base models' predictions. Contrarily, the latter strategies assign different (dynamic) weights to each base model according to its local prediction performance calculated by considering very similar input patterns to the test input pattern under study, such as the nearest neighbors patterns from a validation dataset. In this work, statistics-based strategy is adopted by calculating the median of the individual base models' predictions because it is the simplest to develop and easiest to understand [47], [48].

Once the solar PV production predictions are obtained, this work focuses then on the quantification of the uncertainty that affect the obtained predictions. Specifically, three sources of uncertainties are analyzed in this work: 1) uncertainty due to the model input, i.e., measurement errors of the weather variables; 2) uncertainty due to the inherent variability/stochasticity of the physical process; and 3) uncertainty inherent in the model structure and parameter. In practice, the quantification of the uncertainty entails constructing lower and upper bounds, i.e., Prediction Intervals (*PIs*), of power production values within which the true "a priori unknown" solar PV power production is expected to fall with a predefined confidence level α %, e.g., 90% [49], [50].

Techniques like Bootstrap (BS) [51], Delta [52], Mean-Variance Estimation (MVE) [53], and Lower Upper Bound Estimation (LUBE) [54] were successfully applied for uncertainty quantification in different industrial applications [45], [49], [55]. In this work, the *PIs* are obtained by resorting to the BS technique, as it can be easily integrated to the proposed ensemble approach, in addition to their simplicity, negligible computational efforts required and easiness to understand [49].

As we shall show, the significance of the proposed ensemble approach lies in its capability of:

1) providing more accurate 24h-ahead solar PV power production predictions;
2) providing interval solar PV power production predictions for accommodating the overall uncertainty that affect the solar PV power predictions.

In practice, the improvements in the prediction accuracy and the proper quantification of the corresponding uncertainty, which highlights the discrepancy between the actual/real and the predicted production, can be valuable and informative for the decision maker to properly plan, schedule and control the generation of the available energy sources, ensure the reliability of electric power distribution, for storage system sizing, and for an efficient energy market operation [15], [56], [57].

The proposed approach is verified on a real case study of a grid-connected solar PV system (231 kWac capacity) installed on the rooftop of the Faculty of Engineering at the Applied Science Private University (ASU), Amman, Jordan [58]. The effectiveness of the proposed approach concerning: *i)* the prediction of the power production task, is shown with respect to three well-known performance metrics of literature [25], namely Root Mean Square Error (*RMSE*), Mean Absolute Error (*MAE*), and Weighted Mean Absolute Error (*WMAE*); and *ii)* the quantification of the uncertainty associated with the power predictions, is shown with respect to two well-known performance metrics of literature [49], namely *PI* Coverage Probability (*PICP*) and *PI* Width (*PIW*).

For comparison, smart persistence model and two other benchmark models are used to verify the capability of the proposed approach in providing accurate solar PV power production predictions of the ASU solar PV system. In addition, three approaches of literature, namely the Percentile [59], Kernel Density Estimation (KDE) [60], and the Mean-Variance Estimation (MVE) [49], [53] are used, alternatively, to verify the capability of the proposed approach in quantifying the uncertainty that affect the production predictions obtained by the ensemble for the ASU solar PV system.

Therefore, the major contributions of the present work are:

- The development of a new comprehensive ensemble approach for providing accurate 24h-ahead solar PV power production predictions and quantifying their associated uncertainty in the form of Prediction Intervals (*PIs*) by resorting to the BS technique;
- The comparison and validation of the obtained results with respect to different benchmark cases for the prediction and the uncertainty quantification tasks.

The paper is organized as follows: Section II states the problem. Section III describes the real case study of the ASU solar PV system. Section IV illustrates the proposed ensemble approach for solar PV power production prediction and *PIs* estimation. In Section V, the results of the application of the proposed approach to the real case study are presented and compared with those obtained by other alternative approaches of literature. Finally, some conclusions and future works are given in Section VI.

II. PROBLEM STATEMENT

In this work, it is assumed that the weather data ($\mathbf{W}$) and the corresponding power production data ($\vec{P}$) of a solar PV system for a period of Y years are available. The available weather data include measurements of the ambient temperature ($\overrightarrow{Temp}$) at 1m altitude and the global solar radiation ($\overrightarrow{Irr}$).

The objective of this work is the development of a new comprehensive ensemble approach for the prediction of the 24h-ahead power production of the solar PV system, with the quantification of the associated uncertainty. Specifically, the proposed approach aims at benefiting from deterministic parameters, e.g., the time stamp (in hours) from the beginning of each year data, $T(t, d)$, i.e., the chronological order of time $t, t \in [1, 24]$ at day d of a year, for which the power prediction and the associated uncertainty are to be estimated, and the historical weather values, $\overrightarrow{W}(t, d-i) = [\overrightarrow{Temp}(t, d-i), \overrightarrow{Irr}(t, d-i)]$, collected at time t during the previous i days of day d (i.e., hereafter called embedding dimension), for the following two purposes:

- providing estimates of the solar PV power production at day d (i.e., one day-ahead). In particular, the approach receives in inputs the vector $\vec{x}(t, d) = [T(t, d), \overrightarrow{W}(t, d-i)]$, and provides in output the 24h-ahead prediction of the solar PV power production, $y(t, d) = \hat{P}(t, d), t \in [1, 24]$;
- quantifying the overall uncertainty affecting the solar PV power predictions, $\hat{P}(t, d)$, in the form of a Prediction Interval (*PI*), $PI^{\alpha} = [\hat{P}^{lower}(t, d), \hat{P}^{upper}(t, d)]$, that is an interval of lower and upper power production bounds, $\hat{P}^{lower}(t, d)$ and $\hat{P}^{upper}(t, d)$, respectively, within which the actual power production value, $P(t, d)$, is expected to be with a predefined probability $\alpha\%$, e.g., 80%.

III. CASE STUDY: SOLAR PV SYSTEM

The solar PV system under study is installed at the Applied Science Private University (ASU) in Amman, Jordan at latitude of 32.042044 and at longitude of 35.900232 on the rooftop of Faculty of Engineering, as depicted in Fig. 1. The PV system consists of 14 grid-connected solar inverters, in which 13 inverters are 17 kWac (SMA - STP17000TL-10) and one inverter is 10 kWac (SMA - STP10000TL-10).

FIGURE 1. The 231 kWac PV system installed at the ASU, Amman, Jordan.

FIGURE 2. Weather station and PV system at ASU (retrieved and adapted from Google Maps [61]).

All inverters are with two Maximum Power Point Trackers (MPPT), which allows for design flexibility and optimized performance. For each of the 17 kWac inverters, 3 strings of 20 modules are connected to the first MPPT and one string of 19 modules is connected to the second MPPT. For the 10 kWac inverter, one string of 20 modules is connected to each MPPT. All modules are of the same model (Yingli Solar – YL245-29b) with peak power of 245W, and directly installed over concrete rooftop with 11° tilt angle and 36° azimuth angle (from south to east) [58]. It is worth mentioning that the tilt angle was reduced to 11° for reducing the required distance between PV rows to avoid mutual shading, and this allowed installing more panels. Similarly, panels are oriented with building axis to maximize roof coverage.

The weather (meteorological) data and the associated PV power production are exported from data loggers and monitoring systems of a weather station and of the PV system. The PV system is 171m apart from the weather station, as depicted in Fig. 2 [58].

The meteorological and PV power data are of 1-hour logging intervals, collected during the period from May 16th, 2015 to December 31st, 2016 resulting in 14280 rows of data. The ASU weather station is 36 meter high and equipped with 10 measuring instruments measure the following meteorological parameters (for more details on the ASU solar PV system data, interested readers may refer to [58]):

- Wind speed (at different heights of 10m, 33m, 35m, and 36m) (m/s);
- Wind direction (at different heights of 10m, 33m, 35m, and 36m);
- Soil surface and subsoil temperatures (°C);
- Barometric pressure (hPa);
- Relative humidity (at different heights of 1m and 35m) (%);
- Precipitation amounts (mm);
- Ambient temperature (at different heights of 1m, 33m, and 35m) (°C). The Hygro-Thermo Transmitter with RTD is used for measuring the ambient temperature with high accuracy. The detailed characteristics of the installed Transmitter are reported in Table 1;
- Global and diffuse solar irradiances (W/m^2). Pyranometers are used for measuring the global irradiance, with a high accuracy, on a plane surface resulting from radiant fluxes in the wavelength that span the interval 285 to 2800 nm. The detailed characteristics of the installed Pyranometers are reported in Table 1.

TABLE 1. The detailed characteristics of the installed hygro-thermo transmitter and pyranometers at the ASU weather station.

Hygro-Thermo Transmitter	
Measuring range	-30 to 70°C
Deviation	± 0.2 K
Pyranometers	
Spectral range	285 to 2800nm
Sensitivity	7 to 14μV/W/m^2
Maximum Operational Irradiance	4000W/m^2
Operational Temperature range	-40°C to +80
Detector type	Thermopile

It is worth mentioning that due to the soiling issue in the Jordanian dusty environment, which reduces the efficiency of the PV system; a cleaning program with a frequency of once a week that lasts for 2-3 days has been implemented. Additionally, the system has been cleaned frequently in the winter seasons by the rainfall. This high rate of cleaning indicates the suitability of the collected data in predicting the PV power, while excluding the dust effect.

Among the collected weather features, few features show binary or constant values during the $Y = 1.6$ years period and, thus, they are excluded from the analysis, e.g., precipitation, wind directions, while the remaining weather parameters, e.g., ambient temperature, global solar radiations, are kept in the analysis.

The effect of the remaining weather parameters on the accuracy of the power predictions was investigated in [62]: following a trial-and-errors procedure, different combinations of weather inputs were investigated by developing an optimized ANN as a prediction model. It was found that the combination of the *1)* current time stamp in hours, from the

beginning of each year data, $T(t, d)$, *2)* ambient temperature at height 1m, $\overrightarrow{Temp}(t, d-i)$, *3)* global solar radiation, $\overrightarrow{Irr}(t, d-i)$, measured at time t, $t \in [1, 24]$, in the previous $i = 5$ days (embedding dimension), tends to provide an accurate t-th hour-ahead power production prediction of ASU PV system of day d.

For completeness, it is worth mentioning that body (or cell) temperature was used as input to the prediction model because it has a strong influence on the solar power production predictions [63], [64]. In ASU weather station, this parameter has not been measured. However, several model-based approaches were developed to accurately estimate the cell temperature and compare it with the real (measured) one [65]. Such approaches aim at estimating the cell temperature as a function of solar radiations, ambient temperatures, and PV cell technology dependent nominal operating variables, etc. [65]. For this reason, investigating the effect of the cell temperature on the power predictions becomes crucial if one is interesting to compare the predictability of solar productions of different technologies. In fact, adopting such approaches for estimating the cell temperature and, then, use it for the prediction task, would result in a variable that aggregates the influences of the ambient temperatures and global solar radiations, dominated by the PV cell technology. Thus, this parameter is not taken into account, as far as one PV technology is investigated in this work.

Therefore, the input patterns of the prediction model at the t-th time, $t \in [1, 24]$, can be expressed as:

$$\vec{x}_j(t, d) = [T_j(t, d), \overrightarrow{W}_j(t, d-5), \overrightarrow{W}_j(t, d-4), \times \overrightarrow{W}_j(t, d-3), \overrightarrow{W}_j(t, d-2), \overrightarrow{W}_j(t, d-1)], \quad (1)$$

where $\overrightarrow{W}_j(t, d-i) = [\overrightarrow{Temp_j}(t, d-i), \overrightarrow{Irr_j}(t, d-i)]$, and the corresponding output of the model will be $y_j(t, d) = \hat{P}_j(t, d)$, where $j = 1, \ldots, N$, and N is the overall number of the available data patterns.

For a proper utilization of the dataset for the prediction task, the data are pre-processed as follows [25], [66]:

- incorrect (e.g., negative) solar radiation values and missing associated production values are recognized in early and late daily hours; that can be justified by offset in the solar radiation sensors and inverter failures, respectively. Therefore, the radiation and the production values are set to 0;
- few missing solar radiation, temperature and power production values are recognized in some middle day hours; that can be due to solar radiation and temperature sensors failures and inverter failures or network disruptions, respectively. Therefore, these values are excluded from the analysis;
- the overall data are normalized to the range of [0,1] to improve the training speed and to maintain the correlation between the inputs and, thus, guaranteeing stable convergence of the ANN internal parameters (i.e., weights and biases) [16], [67].

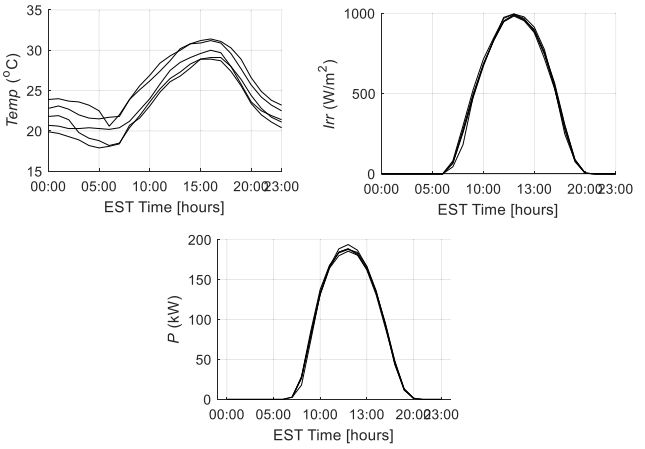

FIGURE 3. Few examples of the pre-processed hourly ambient temperature (top left), global solar radiation (top right), and corresponding solar PV power production (bottom).

For clarification purposes, Fig. 3 shows few examples of the pre-processed hourly ambient temperature at height 1m (top left) and the global solar radiation (top right) and the corresponding solar PV power production (bottom).

The whole inputs/outputs patterns of both the time and the weather features and PV power production, respectively, collected during the $Y = 1.6$ year period are appended in the dataset matrix $\mathbf{X}$ and partitioned into:

- Training datasets, $\mathbf{X}_{train}$: it contains the considered input parameters and the corresponding power production, sampled randomly from May 2015 – August 2016 year data with a fraction of 70%. This dataset (whose generic training pattern vector is denoted as $\vec{x}_{train_j}$, $j = 1, \ldots, N_{train}$) is formed by $N_{train} = 7605$ patterns, which are used for building/training the proposed ensemble prediction approach (Section IV.A);
- Validation dataset, $\mathbf{X}_{valid}$: it contains the considered input parameters and the corresponding power production, sampled randomly from May 2015 – August 2016 year data with the remaining fraction of 30%. A cross validation procedure is employed, as we shall see in the following Sections, for a fair data distribution between the training and validation datasets. This dataset (whose generic training pattern vector is denoted as $\vec{x}_{valid_j}, j = 1, \ldots, N_{valid}$) is formed by $N_{valid} = 3260$ patterns, which are used for optimizing the architectures of the ensemble base models and its configuration (Section IV.B);
- Test dataset, $\mathbf{X}_{test}$: it contains the patterns from September 2016 to December 2016, which have never been used during the development of the ensemble prediction model. This dataset (whose generic training pattern vector is denoted as $\vec{x}_{test_j}, j = 1, \ldots, N_{test}$) is formed by $N_{test} = 2928$ patterns, which are used to evaluate the performance of the developed ensemble prediction approach to other benchmark models like that of the optimum single ANN prediction model.

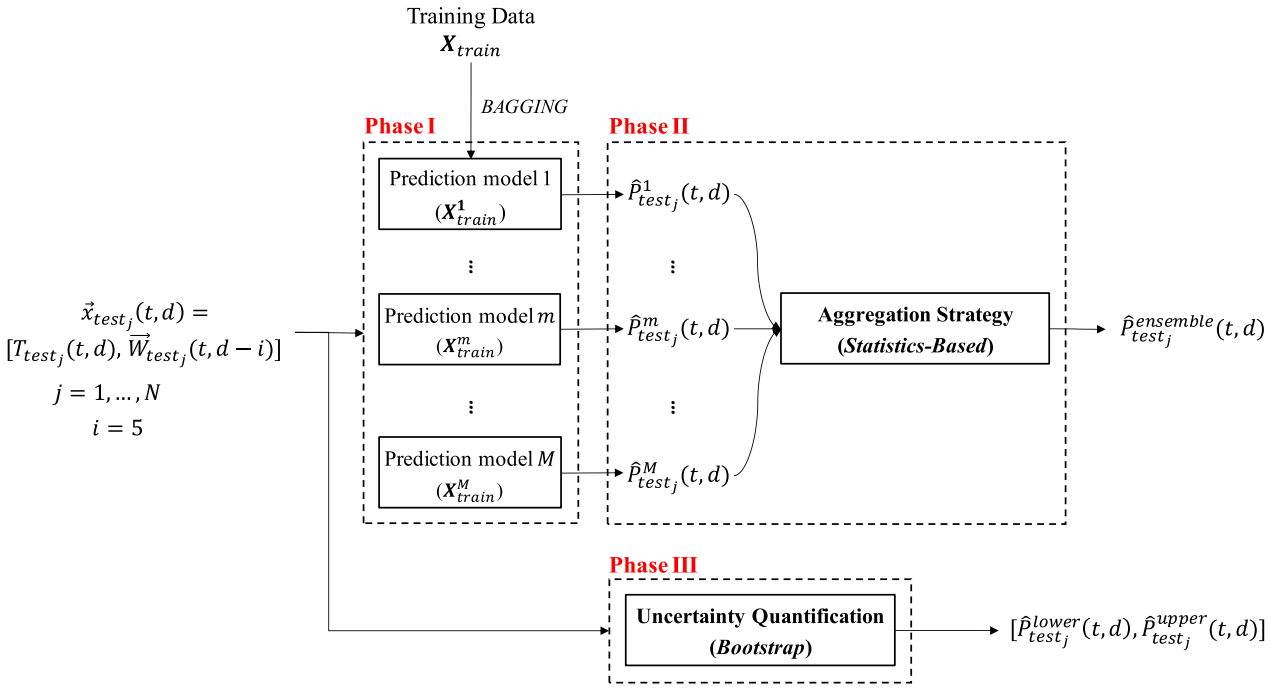

FIGURE 4. Sketch of the proposed data-driven ensemble prediction approach for a solar PV system.

IV. THE PROPOSED APPROACH

In this work, a new comprehensive approach based on an ensemble of M ANNs is developed in a MATLAB environment for two objectives: 1) forecasting the 24h-ahead (i.e., 1 day-ahead) power production of a solar PV system and, 2) quantifying the associated overall uncertainty affecting the 24h-ahead power predictions in the form of *PIs*.

The overall proposed approach entails three Phases and is sketched in Fig. 4. In Phase I, the individual base prediction models of the ensemble are developed and the diversity among the base models is injected by BAGGING technique.

In Phase II, the base prediction models outcomes are aggregated by a statistical-based aggregation strategy into a final solar PV power production prediction (Objective 1) (Section IV.B). In Phase III, the uncertainty associated with the production prediction is quantified by Bootstrap (BS) technique (Objective 2) (Section IV.C).

For a j-th test pattern, $\vec{x}_{test_j}(t,d), j = 1,\dots,N_{test}$, at time t of day d, the proposed approach should 1) provide an estimate of the solar PV power production, $\hat{P}^{ensemble}_{test_j}(t,d)$, and 2) bound the obtained prediction within a *PI* of lower and upper bounds, $\hat{P}^{lower}_{test_j}(t,d)$ and $\hat{P}^{upper}_{test_j}(t,d)$, respectively.

A. INDIVIDUAL DATA-DRIVEN BASE PREDICTION MODELS

Over the last few decades, several data-driven methods were proposed and successfully applied to solar PV power production prediction. For example, Izgi *et al.* [27] applied an ANN to a small scale solar power system (750W) to determine the optimum time horizon for which more accurate short/medium-term power predictions can be obtained; Malvoni *et al.* [68], proposed a Least-Square Support Vector Machine (LS-SVM) for accurate short-term solar power predictions compared to those obtained by the Radial Basis Function Neural Network (RBFNN) of literature; Wolff *et al.* [69], employed the k-nn regression and Support Vector Regression (SVR) for solar PV power predictions on the basis of both measured and forecasted weather conditions.

Although different data-driven methods are shown capable in providing sufficiently accurate solar PV power production predictions, the ANNs are adopted in this work to constitute the proposed ensemble, due to their simplicity, being easy to understand, and due to their capability of successfully solving highly non-linear problems [36], [37], [57]. However, the proposed ensemble approach is general and can be developed by considering any other data-driven methods as base models, like the ELMs and SVMs. This could be an object of a future research work.

ANN is a computational model, originally proposed by [70], inspired by the biological neural networks. ANN consists of several hidden neurons directionally connected by weighted connections structured in a proper architecture of input, hidden (with H hidden neurons) and output layers (Fig. 5) [71], [72]. ANN aims at capturing the hidden complex (a priori unknown) input/output relationship, i.e., current time stamp and historical weather values and the corresponding solar PV power production, respectively: given the training dataset, $\mathbf{X}_{train}$, the ANN should be built/trained on the basis of the available N_{train} training patterns, as follows:

- the input layer receives the j-th vector $\vec{x}_{train_j}(t, d-i)$, $j = 1,\dots,N_{train}$, of the current time stamp (in hours) from the beginning of each year data, $T_{train_j}(t,d)$, and the weather values measured at time t in the previous $i = 5$days of day d, $\overrightarrow{W}_{train_j}(t, d-i)$, from the training dataset, $\mathbf{X}_{train}$;

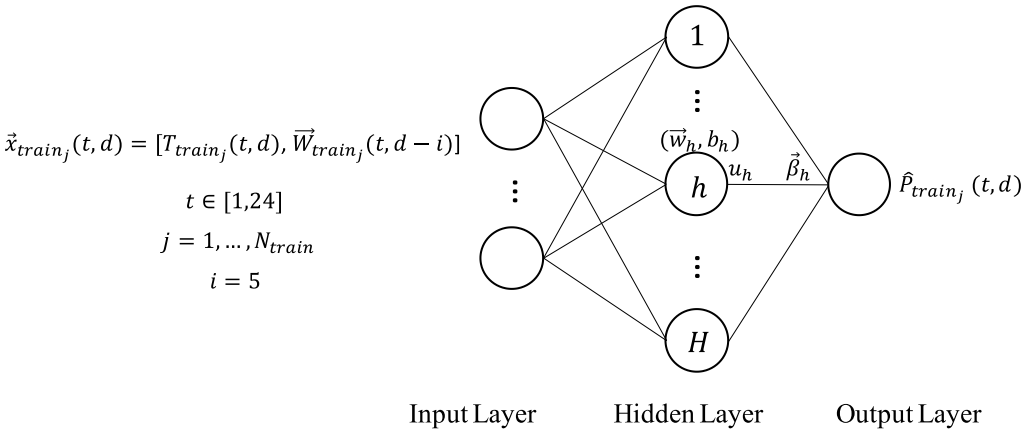

FIGURE 5. ANN model architecture.

- the hidden layer processes the inputs and sends the manipulated information to the output layer via a neuron activation function, G. Specifically, the output of each h-th hidden neuron, u_h, $h = 1, \ldots, H$, is the result of nonlinear transformation (typically sigmoidal), G, of the inputs, $\vec{x}_{train_j}(t,d)$, given by:

$$u_h = G\left(\vec{w}_h.\vec{x}_{train_j}(t,d) + b_h\right), \quad (2)$$

where $\vec{w}_h$ and b_h are the internal parameters of the ANN, namely the weights vector that connects the input nodes to the h-th hidden neuron (it accounts for the effects of the inputs on the target (dependent) variable), and the bias of the h-th hidden neuron, respectively;

- the output layer provides an estimate for the solar PV power production via an output activation function, f. Specifically, the ultimate output is the linear combinations of the H hidden neurons outputs, given by:

$$y_{train_j}(t,d) = \hat{P}_{train_j}(t,d) = \sum_{h=1}^{H} f_h = \sum_{h=1}^{H} \beta_h.u_h, \quad (3)$$

where $\hat{P}_{train_j}(t,d)$ is the predicted solar PV power production at time t of day d and β_h is the output weight that connects the h-th hidden neuron to the output node.

Thanks to the error Back Propagation (BP) learning algorithm, the internal parameters of the ANN (i.e., weights and biases) are initially defined randomly, then updated iteratively to minimize the error between the ANN power production prediction, $\hat{P}_{train_j}(t,d)$, and the actual power production, $P_{train_j}(t,d)$, on the set of training patterns [25], [73]. Examples on the error BP learning algorithms are Levenberg–Marquardt (LM) and Bayesian Regularization (BR) [62], [73]. For more details on the ANN, the interested reader may refer to [74].

Once the ANN is trained, it can be used online to forecast the solar PV power production for any j-th test pattern, $\vec{x}_{test_j}$, $j = 1, \ldots, N_{test}$.

1) GENERATION OF DIVERSE ANN BASE MODELS

Ensemble approaches for solar PV power production prediction task use multiple ANN prediction models and aggregate their prediction outcomes into a final power production prediction. The development of an ensemble entails two steps: 1) building diverse ANN prediction models and 2) aggregating their prediction outcomes by a given strategy of aggregation.

The prediction accuracy provided by an ensemble of multiple models can be improved by generating diversity among its individual base prediction models [39], [40], [57]. The diversity can be typically established by: 1) adopting different prediction techniques (e.g., SVMs, ANNs, k-nn, etc.), 2) adopting the same prediction technique (e.g., ANN), but with different parameter settings (e.g., different numbers of hidden neurons and layers), 3) training each prediction model with different training datasets, by resorting to techniques like boosting [42], Bootstrapping AGGregatING (BAGGING) [40], [41], and Adaboost [43]. For more details on such techniques, the interested reader can refer to [40].

In this work, BAGGING technique is employed to diversify M base ANN models by training each model using a different training datasets, randomly generated using the BAGGING algorithm [41]. Basically, different training datasets are obtained, $\mathbf{X}^m_{train}$, $m = 1, \ldots, M$, by sampling randomly from the original training dataset, $\mathbf{X}_{train}$, with replacement. Therefore, the M training datasets will have the same size, as of the original training dataset, N_{train}.

B. STATIC MEDIAN STRATEGY FOR THE AGGREGATION OF THE INDIVIDUAL ANNS OUTCOMES

Once the ANN prediction models of the ensemble are built, the next step is to develop an effective strategy for aggregating their prediction outcomes. Such strategies can be broadly categorized into statistics-based and model performance-based. The idea underpinning the aggregation strategies is to consider a weight w^m for the solar PV power production prediction, $\hat{P}^m$, obtained by each m-th ANN model, $m = 1, \ldots, M$, and to aggregate their predictions as a weighted average by:

$$\hat{P} = \frac{\sum_{m=1}^{M} w^m.\hat{P}^m}{\sum_{m=1}^{M} w^m}, \quad m = 1, \ldots, M. \quad (4)$$

In statistics-based strategies, typical examples are the Simple Average and the Simple Median aggregation strategies [35]. The former assumes that the weights of all the M predictions of the M ANN models are equal to $w^m = 1/M$, whereas the latter considers only the weight of the center value of the M ANN predictions distribution, i.e., it considers that the weights are all equal to 0 except for the median of the M ANN predictions [35].

In contrary, model performance-based strategies, such as Global Weighted Average and Local Weighted Average, weight the ANN models based on their prediction accuracy estimated on a validation dataset of input-output patterns. For instance, Global Weighted Average assumes that the weights of the ANN models of the ensemble are fixed (equal or not), independently from the test input pattern, based on their performances on a validation dataset, whereas Local Weighted Average adaptively considers that the weight of each ANN model (its contribution to the final aggregated prediction) depends on its local performance evaluated considering a fraction of the input-output patterns of the validation dataset characterized by inputs very similar to that of the input test pattern. In practice, the Local Weighted Average requires the extraction of a fraction of the input patterns from a validation dataset similar to each test input pattern, evaluates the M models performances on that fraction, and assigns the weights to the M models based on their prediction accuracy. This constitutes computational limitations for their deployment in practice, despite the outstanding prediction performance that can be achieved.

In this work, Simple Median aggregation strategy is employed due to its simplicity with no computational limitations [47], [48].

C. BOOTSTRAP (BS) TECHNIQUE FOR UNCERTAINTY QUANTIFICATION

In this Section, the method proposed for the quantification of the solar PV power production prediction in the form of *PIs* is presented. A *PI* with a predefined confidence level, α %, is an interval of lower and upper bounds of the predicted power production at time t, $t \in [1, 24]$ of day d $[\hat{P}^{lower}_{test_j}(t,d), \hat{P}^{upper}_{test_j}(t,d)]$, such that the actual "unknown" value, $P_{test_j}(t,d)$, of the j-th test pattern at time t of day d, falls within the interval with a probability equals to α%:

$$PI^{\alpha} = \left[\hat{P}^{lower}_{test_j}(t,d), \hat{P}^{upper}_{test_j}(t,d)\right],$$
$$Prob\left(\hat{P}^{lower}_{test_j}(t,d) \le P_{test_j}(t,d) \le \hat{P}^{upper}_{test_j}(t,d)\right) = \alpha\%. \quad (5)$$

To this aim, several methods were proposed and applied with success for the estimation of *PIs* on wind power production predictions. To the best of our knowledge, few efforts were dedicated to the development of such methods for the quantification of the uncertainty associated with the solar PV power production predictions, while the focus was on the development of accurate prediction models instead. Examples on methods used for quantifying the uncertainty in different industrial applications are Bootstrap (BS) [51], Delta [52], [55], Lower Upper Bound Estimation (LUBE) [54], and Mean-Variance Estimation (MVE) [53]. In this work, the BS technique is investigated due to the fact that it can easily integrated to the proposed ensemble approach (Section IV.B). It is shown effective for *PI* estimation in various industrial application [49], including wind energy predictions [35], [49].

In solar power predictions, the prediction error variance σ^2_{ε} is decomposed into three error variances associated to the three sources of uncertainty:

- source of uncertainty 1 is due to the errors in the model input (i.e., measurement errors of the weather variables) (σ^2_W);
- source of uncertainty 2 is due to the inherent variability (stochasticity) of the physical process (i.e., similar weather conditions might entail some differences in the solar PV power production) (σ^2_{PR});
- source of uncertainty 3 is due to the ANN model error (i.e., due to different parameter settings of the ANN and/or different training datasets used for building/developing the ANN models) (σ^2_{MO}).

The prediction error variance, σ^2_{ε}, is, then, defined by:

$$var\,[\varepsilon] = \sigma^2_{\varepsilon} = \sigma^2_W + \sigma^2_{PR} + \sigma^2_{MO}. \quad (6)$$

The flowchart of the BS technique for the estimation of the unknown σ^2_{ε}, and the associated *PIs*, is sketched in Fig. 6. There are two steps:

Step 1: Building the BS training dataset. Let us assume that a dataset of weather data and their associated power production, $\mathbf{X} = [\mathbf{W}, \vec{P}]$, are available. This dataset is portioned in two datasets: a training dataset $\mathbf{X}_{train} = [\mathbf{W}_{train}, \vec{P}_{train}]$ for building the ANN ensemble models and a validation dataset $\mathbf{X}_{valid} = [\mathbf{W}_{valid}, \vec{P}_{valid}]$ for providing estimates of the power production, $\hat{P}_{valid}$, whose true production $\vec{P}_{valid}$ are already known. The BS training dataset $\mathbf{X}^{BS}_{train} = [\mathbf{W}_{valid}, \left(\vec{P}_{valid} - \vec{\hat{P}}_{valid}\right)^2 - \vec{\sigma}^2_{MO_{valid}}]$ can then be prepared with the weather-forecasting data of the validation dataset, $\mathbf{W}_{valid}$, and the squared prediction errors, $\left(\vec{P}_{valid} - \vec{\hat{P}}_{valid}\right)^2 - \vec{\sigma}^2_{MO_{valid}}$, excluding the model error, on the validation dataset. It is important to point out that this term includes the source of uncertainty 1 and 2 [35].

Step 2: Constructing the BS PIs of the test pattern. With the BS training dataset, a dedicated feedforward ANN is developed for providing, at time t, an estimate of the variance, $\sigma^{2_{test_j}}_{\varepsilon} = \sigma^{2_{test_j}}_W + \sigma^{2_{test_j}}_{PR} + \sigma^{2_{test_j}}_{MO}$, associated of a general test pattern of weather data, $\vec{W}_{test_j}$. To ensure a strictly positive variance estimate, an exponential activation function is used [45], [49].

Finally, the *PI* of the test pattern at time t with a confidence level of α% can be obtained by [53], [75]:

$$\left[\hat{P}^{lower}_{test_j}(t,d), \hat{P}^{upper}_{text_j}(t,d)\right] = \hat{P}_{test_j}(t,d) \pm C^{\alpha}_{dof}.\sigma^{2_{test_j}}_{\varepsilon}(t,d), \quad (7)$$

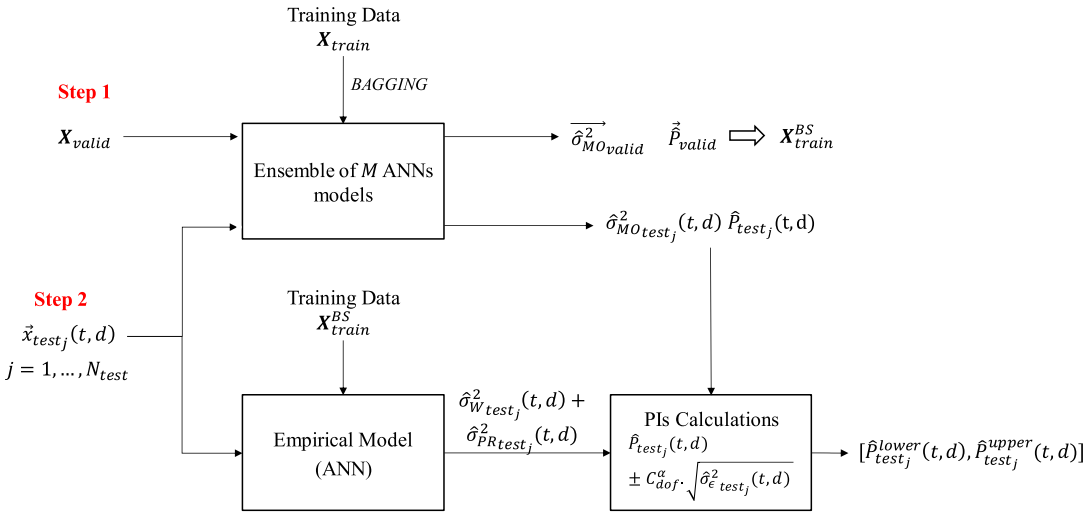

FIGURE 6. Scheme of the BS technique for estimating PIs of solar PV power production predictions.

TABLE 2. The detailed characteristics of each ANN base model in the proposed ensemble.

Characteristics	Description
Configuration	11-31-1
Number of hidden neurons	$H^{opt} = 31$
Performance function	MSE
Activation function (hidden layer)	Log-sigmoid
Activation function (output layer)	Purlin
Training algorithm	LM

where $\hat{P}_{test_j}$ is the power production predicted by the ANN ensemble for the test pattern at time t and C^{α}_{dof} is the (1-α)/2 quantile of a Student t-distribution with degrees of freedom (*dof*) equal to the number of ensemble models H [35].

V. APPLICATION OF THE PROPOSED ENSEMBLE APPROACH TO THE REAL CASE STUDY

The effectiveness of the proposed ensemble approach for solar PV power production prediction and uncertainty quantification is demonstrated by the real case study of Section III in Section V.A and Section V.B, respectively. The obtained results are compared to those obtained by smart persistence model as a *Baseline* and two other benchmark models for the prediction task (Section V.A) and three approaches used alternatively for the uncertainty quantification task (Section V.B).

A. ENSEMBLE POWER PRODUCTION PREDICTION

An ensemble of M ANN models is developed in which the diversity among the models is generated by using the BAGGING technique. Each ANN model is assumed to be characterized by an architecture of input, hidden and output layers. The ANN models are built in MATLAB environment by resorting to the LM error BP learning algorithm. The detailed characteristics of each m-th ANN model of the ensemble, $m = 1, \ldots, M$, are reported in Table 2.

The optimum number of hidden neurons, H, in the hidden layer and the optimum number of the ANN ensemble models, M, are selected according to the ensemble prediction accuracy obtained on the N_{valid} input-output validation patterns by a trial-and-error procedure. To this aim, eight possible numbers of the hidden neurons, $H^{candidate} = 1, 6, 11, 16, 21, 26, 31, 36$ and five possible numbers of the ensemble models, $M^{candidate} = 1, 10, 20, 40, 60$, are considered.

The Root Mean Square Error (*RMSE*) (in kW) is considered for the quantification of the ensemble prediction accuracy for the different combinations of $H^{candidate}$ and $M^{candidate}$. The *RMSE* is the average production prediction error, i.e., small *RMSE* values indicate more accurate predictions. *RMSE* is defined by [16], [25], [57]:

$$RMSE = \sqrt{\frac{\sum_{j=1}^{N_{valid}} \left(\hat{P}_j - P_j\right)^2}{N_{valid}}}. \quad (8)$$

To robustly evaluate the ensemble prediction performance in terms of the *RMSE*, a 5-fold cross-validation procedure is carried out. In practice, we sample the training and the validation patterns randomly 5 different times (5-fold) from the data in the period May 2015-August 2016 with a fraction of 70% and 30%, respectively. The final *RMSE* value is then, computed by simply averaging the 5 *RMSE* values. In fact, one can employ advanced meta-heuristic optimization algorithms, such as Particle Swarm Optimization (PSO) [76], [77], Cuckoo Search (CS) [78], Genetic Algorithm (GA) [76], or a combination of these algorithms, to define optimally the ANN base models internal parameters (e.g., number of hidden neurons, activation functions, etc.) and the number of ensemble models, while avoiding the traditional iterative BP algorithm. As far as the objective of this work is to show the powerful of the ensemble in accurately predicting the solar power production and properly quantifying the associated uncertainty with convenient

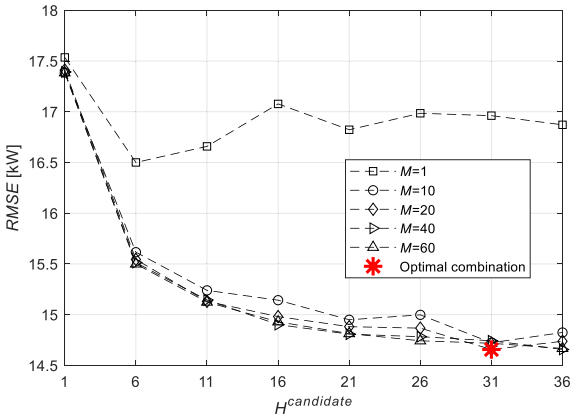

FIGURE 7. *RMSE* values for different combinations of number of hidden neurons (H) and number of models of the ensemble (M).

computational efforts (as we shall see later); the utilization of the basic trial-and-error procedure is sufficient.

Fig. 7 shows the *RMSE* values obtained by the application of the ensemble characterized by the different combinations of $H^{candidate}$ and $M^{candidate}$.

One can conclude the following:

- As long as number of models that compose the ensemble, M, and number of hidden neurons, H, increase; the prediction accuracy increases (i.e., *RMSE* decreases). This enhancement is more noticeable when the ensemble comprises $M \geq 20$ models and the models comprise $H \geq 31$;
- Further increments in number of models and of hidden neurons of the ensemble models entail non-significant improvements in the prediction accuracy. This combination can be avoided for reducing the computational efforts and ensemble complexity;
- The optimal combination can be considered when the ensemble comprises $M^{opt} = 20$ with $H^{opt} = 31$ hidden neurons (star marker).

It is worth mentioning that the proposed ensemble approach has been performed with a Matlab code that has been in-house developed and that the computational time needed to optimize the architectures of the ensemble base models (i.e., $H^{candidate}$) and its configuration (i.e., $M^{candidate}$) with 5-fold cross validation on an Intel Core i7 is 79.62 minutes. It is, indeed, expected that as long as number of ensemble models increases (1, 10, 20, 40, 60), the computational efforts required for building the ensemble would increase too (∼37, 336, 666, 1243, 2495 seconds, respectively). Thus, a trade-off between the computational efforts, ensemble complexity, and the prediction accuracy is necessary.

Once the ensemble configuration and its ANNs architectures are defined, it is applied on the test dataset, $\mathbf{X}_{test}$, and its prediction performance is evaluated on the N_{test} input-output test patterns by considering the following three performance metrics [16], [30]:

- the *RMSE* (3);
- the Mean Absolute Error (*MAE*) (in kW), i.e., the average error of the solar PV power production prediction. It is defined by (9):

$$MAE = \frac{\sum_{j=1}^{N_{test}} \left| \left(\hat{P}_j - P_j \right) \right|}{N_{test}}, \tag{9}$$

- the Weighted Mean Absolute Error (*WMAE*), i.e., the average relative error of the solar PV power production prediction. It is defined by (10):

$$WMAE = \frac{\sum_{j=1}^{N_{test}} \left| \left(\hat{P}_j - P_j \right) \right|}{\sum_{j=1}^{N_{test}} P_j}, \tag{10}$$

where $\hat{P}_j$ and P_j are the predicted and the true solar PV power production, respectively, of each j-th test patterns, $j = 1, \ldots, N_{test}$. Small *RMSE*, *MAE* and *WMAE* values entail accurate power predictions.

Table 3 summarizes the three performance metrics obtained by the proposed ensemble approach with respect to those obtained by three benchmark models, along with the time required for building and evaluating the models using the training and test datasets, respectively:

- *Benchmark 1* (Smart Persistence [79]): in which the production at time t over the 24 hours prediction horizon, $\Delta t = 24$ (one day-ahead prediction) is assumed to be the same as of the recent production measured in the previous day at the same time t, $\hat{P}_{t+\Delta t} = P_t$, $t \in [1, 24]$. This model is usually considered as a *Baseline*-forecasting model and it is used to evaluate the effectiveness of any other developed models for forecasting.
- *Benchmark 2* (Average of $M = 20$ ANNs): in which the final performance metrics are the average values of the three performance metrics obtained by the 20 ANNs of

TABLE 3. Performance of the proposed ensemble approach and the three benchmark models on the test dataset.

Prediction Strategy	*RMSE* [kW]	pg_{RMSE} [%]	*MAE* [kW]	pg_{MAE} [%]	*WMAE*	pg_{WMAE} [%]	Training time [sec]	Test time [sec]
Benchmark 1 (Baseline) **(Smart Persistence)**	14.12	0	6.99	0	0.136	0	0	0.06
Benchmark 2 **(Average of 20 ANNs)**	14.41	-2.07%	7.19	-2.30%	0.144	-5.81%	32.06	0.38
Benchmark 3 **(Best of 20 ANNs)**	13.06	7.46%	6.42	8.19%	0.13	5.07%	1.69	0.02
The proposed approach **(Ensemble)**	**12.61**	**10.70%**	**6.15**	**12.10%**	**0.12**	**9.12%**	**32.06**	**0.38**

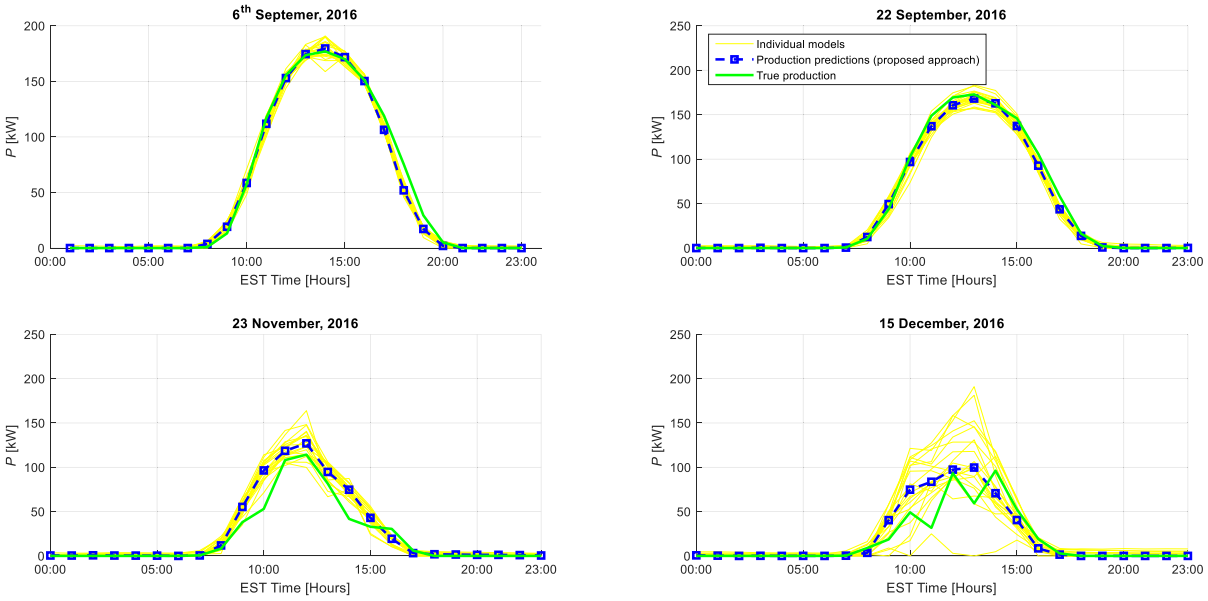

FIGURE 8. Few examples of power production predictions obtained by the proposed ensemble approach together with those obtained by the individual 20 ANNs models.

the ensemble. This is typically the current case of the ASU PV system [62], [66];

- *Benchmark 3* (Best of $M = 20$ ANNs): in which the final performance metrics are those obtained by the best ANN model among the 20 available models of the ensemble.

In order to evaluate the performance gain obtained by the application of the proposed ensemble approach, the performance gain ($pg_{Metric}\%$) of the proposed ensemble approach with respect to the *Baseline*smart persistence model is calculated. The performance gain can be computed for the three metrics by [57]:

$$pg_{Metric}\,(\%) = \left(\frac{METRIC^{Baseline} - METRIC^{Ensemble}}{METRIC^{Baseline}}\right) * 100. \tag{11}$$

Notice that, positive performance gains of the three metrics entail that the forecasting approach that in need to be verified outperforms the *Baseline* smart persistence forecasting model (as in the case of the proposed ensemble approach), and vice versa (as in the case of the Benchmark 2).

Looking at Table 3, one can notice that the proposed ensemble approach significantly improves the accuracy of the power production predictions compared to the benchmark models including the *Baseline* smart persistence model. In fact, one can notice that the performance of the individual ANN models (Benchmark 2 – average of 20 ANN models) is less than that of the smart persistence model that justified the impact of the proposed ensemble approach. In practice, the benefits of such improvements should be evaluated by considering other factors, like the delivered versus scheduled power production, imbalance costs and penalties, and ancillary service costs. For large scale PV systems, one can also consider the market participation and potential emissions implications [24], [80], [81].

In addition, one can notice that the proposed approach, despite its nature as an ensemble of prediction models, necessitates short training/test time (i.e., 32.06 and 0.38 seconds, respectively) that would increase its potentiality in real time applications. Indeed, the times necessary to establish the *Baseline* model and the single (best) ANN model are negligible compare to the proposed approach: the former requires no training due to its nature, whereas the latter is a single model and would be obtained after a trial-and-error procedure among several other ANN models. However, their accuracies are worse than those obtained by the proposed approach that makes it worthy to be proposed. Future works can be devoted towards investigating other base prediction models, such as Extreme Learning Machines (ELMs), that prove their simplicity, fast computational and good generalization capability in similar applications, to further enhance the proposed ensemble approach [25].

Fig. 8 shows few examples of the 24h-ahead power predictions obtained by the proposed ensemble approach (squares) along with those obtained by the 20 individual ANNs models (light shade of color) for two clear (6 September, 2016 and 22 September, 2016) and cloudy (23 November, 2016 and 15 December, 2016) days. It can be seen that:

1) the power production predictions provided by the proposed ensemble are reasonably close to the true power production, in particular for the two clear days. The predictions are less accurate in the two cloudy days due to the extreme conditions experienced by the ASU PV system. In fact, one might be wondering whether considering the cloudy hours as an additional input to the proposed approach can further enhance the predictability of the solar PV power. However, from the point of view that the clouds have the largest impact on surface level solar radiation and, thus, their effect

is already embedded in the level of solar radiation received by the solar radiation sensor.

2) the variability (uncertainty) of the individual models' predictions is large at the middle of the day (due to the large variability of the weather conditions experienced by the ASU PV system) with respect to that shown at the early morning and late evening time hours (due to the small variability of the weather conditions experienced by the ASU PV system). This remark will be explained further in Section V.B through the quantification of the uncertainties that affect the power production predictions.

In conclusions, one of the strengths of the proposed ensemble approach lies in its capability of benefiting from the strengths while overcoming the drawbacks of the diverse 20 ANNs models. Thus, their aggregation improves upon the performance of each sole ANN model. It is worth mentioning that the impact of the proposed approach can be greatly significant if it is applied towards minute-ahead forecasting for which time series modeling is much more relevant. This can be an object of future research work.

B. POWER PRODUCTION PREDICTION UNCERTAINTY

In this Section, the *PIs* obtained by the developed ensemble approach of Section V.A on the test data, $\mathbf{X}_{test}$, are presented and compared with those obtained by three other approaches used, alternatively, to quantify the associated uncertainty of the power predictions obtained by the ensemble, $\hat{P}^{ensemble}(t,d)$, at time t of day d. They are:

1) **Percentile (quantile) technique** [59]. It computes the percentiles (quantiles) of the M predicted power production obtained by the M models of the ensemble, $\hat{P}^m(t,d)$, $m = 1,..,M$. In this work, the 10^{th} and 90^{th} percentiles for the lower, $\hat{P}^{lower}(t,d)$, and upper, $\hat{P}^{upper}(t,d)$, bounds, of the *PI*, respectively, are calculated for a confidence level of $\alpha = 80\%$;

2) **Non-parametric Kernel Density Estimation (KDE) technique** [60]. It estimates the Probability Density Function (PDF) of the power predictions obtained by the M models of the ensemble, $\hat{P}^m(t,d)$, $m = 1,..,M$. Basically, it sums the Gaussian kernel functions assigned to each of the m-th power prediction to obtain the final PDF, whose 10^{th} and 90^{th} percentiles are the lower, $\hat{P}^{lower}(t,d)$, and upper, $\hat{P}^{upper}(t,d)$, bounds, of the *PI*, respectively. More details about the KDE can be found in [60].

3) **Mean Variance Estimation (MVE) technique** [53]. It assumes that the prediction error obtained by the ensemble, i.e., $\varepsilon = P - \hat{P}^{ensemble}$, for an input test pattern, is an uncertain variable distributed according to a Gaussian distribution function whose variance σ_ε^2 has to be estimated, by using a dedicated ANN properly developed with a procedure similar to that followed for the BS technique [53]. The dependence of this variance on the input test patterns is the key assumption of the MVE. In this work, an ANN with three layers and 100 hidden neurons is built for establishing the 80% *PIs* of the power production predictions obtained by the ensemble. Briefly, MVE aims at preparing a training dataset $\mathbf{X}_{train}^{MVE} = [\mathbf{W}_{valid}, \left(\vec{P}_{valid} - \vec{\hat{P}}_{valid}\right)^2]$, that comprises the inputs weather data of the validation dataset, $\mathbf{W}_{valid}$, and the squared prediction errors, $\left(\vec{P}^{valid} - \vec{\hat{P}}^{valid}\right)^2$, obtained on the validation dataset. Once the training dataset is constructed, the dedicated ANN is built for providing, at time t, an estimate of the variance, $\sigma_\varepsilon^{2_{test_j}}$ (3), associated of a general test pattern of weather-forecasting data, $\overrightarrow{W}_{test_j}$. The 80% *PIs* can be, then, estimated by resorting to (4). To ensure a strictly positive variance estimate, an exponential activation function is used. More details on the MVE can be found in [49], [53].

To this aim, dedicated feedforward ANNs characterized by an architecture of three layers (input, hidden and output) and 7 hidden neurons are developed for the estimations of the prediction error variance in the MVE and the BS techniques.

The estimated *PIs* are evaluated with respect to two well-known performance indicators [49], [82]. The objective of a *PI* with confidence $\alpha\%$ is to have coverage of at least $\alpha\%$ with width as small as possible [83]: *1)* the *PI* Coverage Probability (*PICP*), i.e., the fraction of true production that falls within the computed *PIs* and *2)* the *PI* Width (*PIW*) (in kW).

TABLE 4. *PIs* Performances obtained by the proposed approach and the three alternative approaches on the test dataset, for $\alpha = 80\%$ target confidence level.

Prediction Intervals for α=80%	*PICP*	*PIW* [kW]
Percentile	0.64	10.49
KDE	0.81	24.10
MVE	0.82	25.61
The proposed approach (BS)	**0.84**	**26.13**

Table 4 reports the *PIs* average performances over the 50-fold cross validations obtained by the proposed approach and the three other alternative approaches in terms of *PICP* and *PIW*.

One can easily recognize that the *PIs* obtained by the percentile technique are the narrowest (*PIW*) but have very low coverage value ($PICP = 0.64$), which is less than the target coverage level of 0.8. On the other hand, the other approaches provide larger (and to some extent similar) *PIs* widths, therefore, acceptable (and to some extent similar) coverage values (with respect to the target coverage level of 0.8). Specifically, the *PIs* provided by the BS technique are the widest, leading to large coverage probability. For instance, with respect to the MVE technique, the larger *PI* widths obtained by the BS technique can be justified by the fact that it considers the uncertainty inherent in the model structure and parameter, whereas the MVE technique does not, and thus, narrower *PIs* are expected to be obtained by the MVE than the BS, leading to lower coverage levels [49], [84].

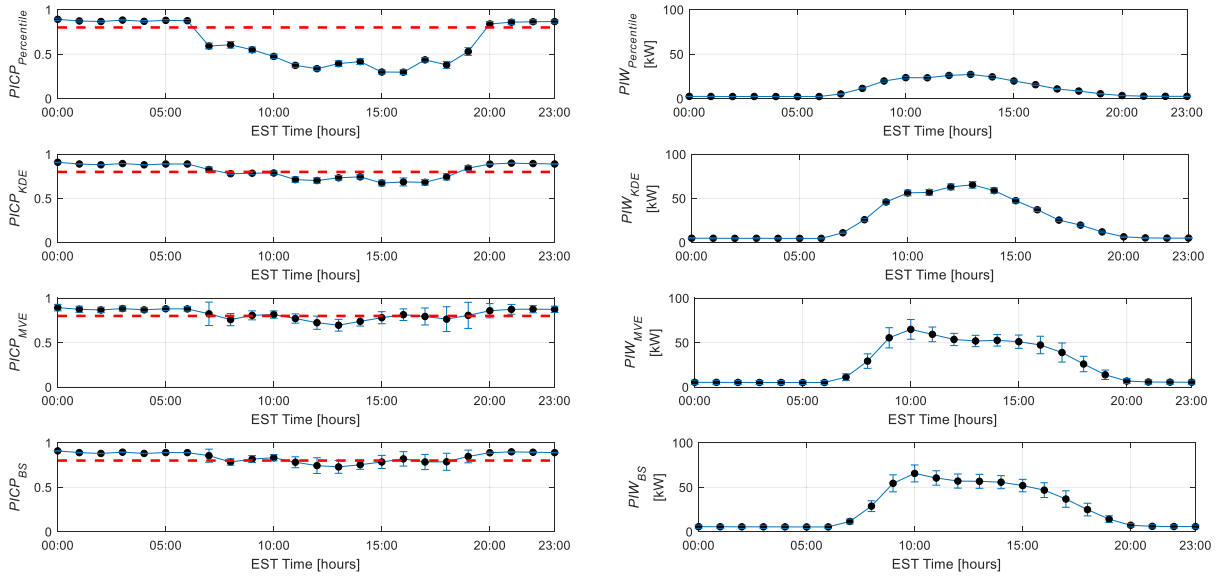

FIGURE 9. Overall average coverage (left) and PI width (right) of the Percentile (top), KDE (middle top), MVE (middle bottom), and the proposed approach (bottom).

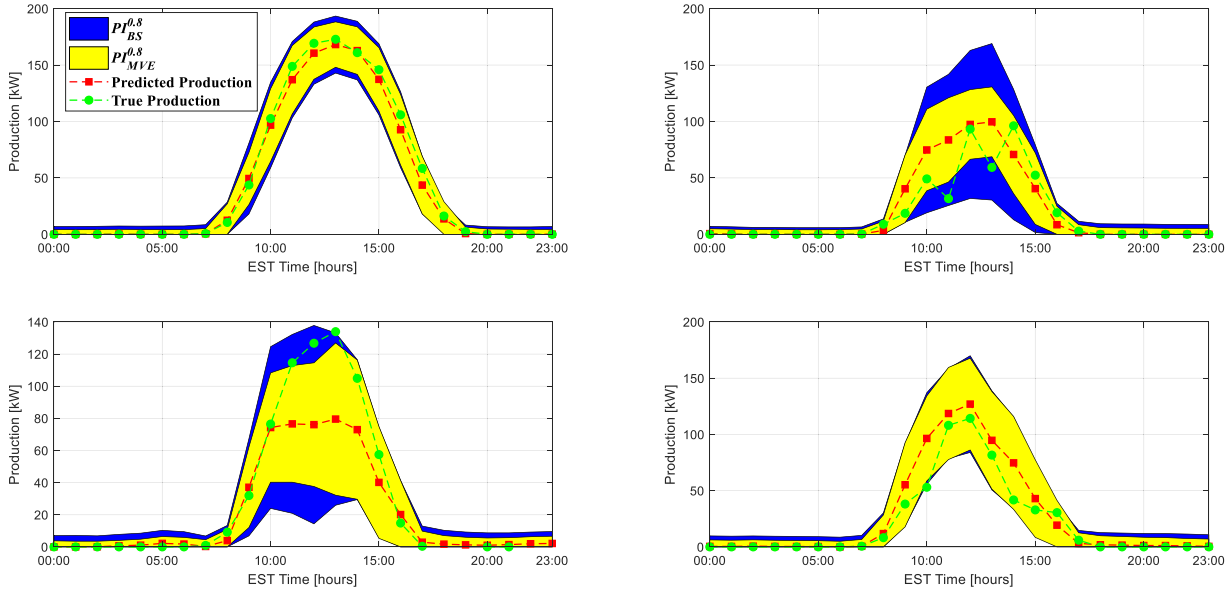

FIGURE 10. Comparison of the PIs obtained by the proposed approach (dark shade of color) and the MVE (light shade of color).

To further compare these approaches, in depth analysis is performed in which the hourly *PIs* performances (i.e., from 00:00 to 23:00, EST) are computed and compared as shown in Fig. 9. Fig. 9 (left) shows the overall average values of the *PICP*, whereas Fig. 9 (right) shows the corresponding average values of the *PIW*, with the standard deviations computed for both metrics over the 50-fold cross validations, obtained by the percentile (top), KDE (middle top), MVE (middle bottom) and the proposed approach (bottom). One can notice the following:

- the *PIs* obtained by the Percentile technique are the narrowest among the other techniques (Fig. 9 (right top)) but does not have acceptable coverage values, less than the target coverage level of 0.8 (Fig. 9 (left top));
- the *PIs* obtained by the aforementioned techniques are narrow for early morning and late evening day hours (Fig. 9 (right)) with acceptable coverage levels (higher than 0.8) (Fig. 9 (left)). The *PIs* in the middle hours of the day are expanded to accommodate the high variability (stochasticity) of the weather conditions;
- the *PIs* obtained by the KDE are slightly narrower than those obtained by the MVE and BS techniques, but they fail to satisfy the target coverage level for most of the middle time hours;

- the *PIs* provided by the BS technique are wider than those obtained by the MVE technique, which leads to a large coverage probability, satisfying the target coverage level at all-time instances, e.g., MVE fails to achieve the 0.8 coverage level at 13:00, whereas the BS does;
- In addition, the variability represented by the standard deviations of the coverage probability using the BS technique (Fig. 9 (left bottom)) is smaller than those obtained by the MVE technique (Fig. 9 (left middle bottom)).

For clarification purposes, Fig. 10 shows few examples of the *PIs* obtained by the proposed approach (i.e., BS) (dark shade of color) along with those obtained by, for instance the MVE approach (light shade of color). In addition. Fig. 10 shows the true and the predicted solar PV power production obtained by the ensemble approach of Section IV (circles and squares, respectively).

It can be seen that the *PIs* provided by the BS approach are expanded to accommodate the variability in the weather conditions and, thus, satisfying the target coverage level of 0.8 at most of the time instances of the four different examples (days) with respect to those obtained by the MVE approach of literature.

In conclusion, the BS technique is superior to the other alternative approaches in achieving the target coverage level of 0.8 at all-time instances of the day with marginally wider *PIs* widths than the best alternative techniques, the KDE and the MVE.

VI. CONCLUSIONS AND FUTURE WORKS

In this work, an ensemble of optimized and diversified Artificial Neural Networks (ANNs) for 24h-ahead predicting the solar PV power production and, at the same time, quantifying the associated uncertainty that affect the power production predictions is proposed.

The main contributions in this work are: *i)* the development of a new comprehensive ensemble approach for providing accurate 24h-ahead solar PV power production predictions and quantifying their associated uncertainty in the form of Prediction Intervals (*PIs*) by resorting to the Bootstrap (BS) technique; *ii)* the comparison and the validation of the obtained results with respect to smart persistence model and two other cases of a single optimized ANN model for the prediction task, and of the Percentile, Kernel Density Estimation (KDE), and the Mean-Variance Estimation (MVE) techniques of literature for the uncertainty quantification task.

The ANNs base models of the proposed ensemble are optimized in terms of number of hidden neurons in the hidden layer by a trial-and-error procedure and diversified by resorting to BAGGING technique.

Standard performance metrics are considered to evaluate the effectiveness of the proposed approach with respect to the benchmark approaches, they are: *i)* the performance gains of the Root Mean Square Error (*RMSE*), Mean Absolute Error (*MAE*), and Weighted Mean Absolute Error (*WMAE*) for the quantification of the predication accuracy gain, and *ii)* the *PI* Coverage Probability (*PICP*) and *PI* Width (*PIW*) for the quantification of the goodness of the obtained *PIs*.

The proposed approach is verified with respect to a real case study regarding a grid-connected solar PV system (231 kWac capacity) installed on the rooftop of the Faculty of Engineering at the Applied Science Private University (ASU), Amman, Jordan. Results show the superiority of the proposed approach in providing accurate 24-h power production predictions with a reduction in terms of *RMSE*, *MAE*, and *WMAE* up to 11%, 12%, and 9%, respectively, while robustly quantifying different sources of uncertainty that affect the production predictions. Finally, we believe that the proposed approach can be considered as a comprehensive approach from which the solar energy plants can be benefit in enhancing the solar power productions predictions and, at the same time, accommodate the uncertainty that can influence the predictions.

Future works will be devoted towards *i)* the implementation of advanced data-driven techniques as base models of the ensemble, such as Extreme Learning Machines (ELMs) and Echo State Networks (ESNs), *ii)* the development of advance ensemble aggregation strategies, such as the Local Fusion strategy, and *iii)* to further optimize the base models (in terms of their internal parameters) by using advanced optimization techniques like Particle Swarm Optimization (PSO), Cuckoo Search (CS) optimization, and Genetic Algorithms (GAs), to further enhance the prediction accuracy.

NOMENCLATURE

A. ABBREVIATIONS

RE	Renewable Energy
PV	Photovoltaics
LCOE	Levelised Cost Of Electricity
ANNs	Artificial Neural Networks
BP	Back Propagation
LM	Levenberg–Marquardt
BR	Bayesian regularization
GBRT	Gradient Boosting Regression Trees
RBFNN	Radial Basis Function Neural Network
SVMs	Support Vector Machines
LS-SVM	Least-Square Support Vector Machine
SVR	Support Vector Regression
ELMs	Extreme Learning Machines
MME	Multi-Model Ensemble
k-nn	k-nearest neighbors
PIs	Prediction Intervals
BAGGING	Bootstrapping AGGregatING
BS	Bootstrap
MVE	Mean Variance Estimation
KDE	Kernel Density Estimation
LUBE	Lower Upper Bound Estimation
ASU	Applied Science Private University
MPPT	Maximum Power Point Trackers
PSO	Particle Swarm Optimization
CS	Cuckoo Search optimization
GA	Genetic Algorithm

B. NOTATIONS

$\mathbf{W}$	Overall weather data
$\vec{P}$	Overall power production data
Y	Number of available years data
$\overrightarrow{Temp}$	Overall ambient temperatures vector
$\overrightarrow{Irr}$	Overall global solar radiations vector
t	Time instant, $t \in$[1,24]
d	Index of a day
i	Embedding dimension
$\vec{W}(t, d-i)$	Overall weather conditions vector collected at time t from previous i days of day d
$\vec{x}(t, d)$	Overall input vector to the prediction model collected at time t of day d
$y(t, d)$	Production prediction obtained at time t of day d
$P(t, d)$	True production at time t of day d
$\hat{P}(t, d)$	Production prediction obtained at time t of day d
$\hat{P}^{lower}(t, d)$	Lower production prediction obtained at time t of day d
$\hat{P}^{upper}(t, d)$	Upper production prediction obtained at time t of day d
α	Target confidence level
PI^{α}	Prediction Interval of confidence α
N	Number of available input-output patterns
N_{train}	Number of training input-output patterns
N_{valid}	Number of validation input-output patterns
N_{test}	Number of test input-output patterns
j	j-th input-output pattern, $j = 1, \ldots, N$
$T_j(t, d)$	Time stamp of a generic j-th pattern collected at time t of day d
$\overrightarrow{Temp_j}(t, d-i)$	Ambient temperature vector of a generic j-th pattern collected at time t from previous i days of day d
$\overrightarrow{Irr_j}(t, d-i)$	Global solar radiations vector of a generic j-th pattern collected at time t from previous i days of day d
$\vec{W}_j(t, d-i)$	Weather conditions vector of a generic j-th pattern collected at time t from previous i days of day d
$\vec{x}_j(t, d)$	Input vector to the prediction model of a generic j-th pattern collected at time t of day d
$P_j(t, d)$	True production of a generic j-th pattern at time t of day d
$\hat{P}_j(t, d)$	Production prediction of a generic j-th pattern at time t of day d
$\mathbf{X}$	Input-output overall dataset
$\mathbf{X_{train}}$	Input-output training dataset
$\mathbf{X_{valid}}$	Input-output validation dataset
$\mathbf{X_{test}}$	Input-output test dataset
$\vec{x}_{test_j}$	Generic test pattern vector, $j = 1, \ldots, N_{test}$
$\vec{x}_{valid_j}$	Generic validation pattern vector, $j = 1, \ldots, N_{valid}$
$\vec{x}_{train_j}$	Generic training pattern vector, $j = 1, \ldots, N_{train}$
M	Number of prediction models of the ensemble
m	Index of prediction model, $m = 1, \ldots, M$
$M^{candidate}$	Possible number of models in the ensemble
M^{opt}	Optimum number of models in the ensemble
$T_{test_j}(t, d)$	Time stamp (in hours) of the j-th test pattern
$\overrightarrow{Irr}_{test_j}(t, d-i)$	Global solar radiations vector of the j-th test pattern collected at time t from previous i days of day d
$\overrightarrow{Temp}_{test_j}(t, d-i)$	Ambient temperature vector of the j-th test pattern collected at time t from previous i days
$\vec{W}_{test_j}(t, d-i)$	Weather conditions vector of the j-th test pattern collected at time t from previous i days of day d
$\vec{x}_{test_j}(t, d)$	Input vector to the prediction model of the j-th test pattern collected at time t of day d
$\hat{P}^{m_j}_{test}(t, d)$	m-th production prediction of the j -th test pattern obtained at time t of day $d, j = 1, \ldots, N_{test}$
$\hat{P}^{ensemble}_{test_j}(t, d)$	Ensemble production prediction of the j-th test pattern obtained at time t of day $d, j = 1, \ldots, N_{test}$
$\hat{P}^{lower}_{test_j}(t, d)$	Lower production prediction of the j-th test pattern obtained at time t of day $d, j = 1, \ldots, N_{test}$
$\hat{P}^{upper}_{test_j}(t, d)$	Upper production prediction of the j-th test pattern obtained at time t of day $d, j = 1, \ldots, N_{text}$
$\mathbf{X^m_{train}}$	m-th training dataset used for training m-th ANN
H	Number of hidden neurons
h	Index of hidden neuron, $h = 1, \ldots, H$
$H^{candidate}$	Possible number of hidden neurons
H^{opt}	Optimum number of hidden neurons
$\vec{W}_{train_j}(t, d-i)$	Weather conditions vector of the j-th training pattern collected at time t from previous i days of day d
$\vec{x}_{train_j}(t, d)$	Input vector to the prediction model of the j-th training pattern collected at time t of day d

G	Neuron activation function
u_h	Output of each h-th hidden neuron, $h = 1, \ldots, H$
$\overrightarrow{w}_h, b_h$	Internal parameters of the ANN
f_h	Output activation function from the h-th neuron
β_h	Output weight that connects the h-th hidden neuron to the output node
$y_{train_j}(t, d)$	Production Prediction of a j-th training pattern at time t of day d
$P_{train_j}(t, d)$	True production of a j-th training pattern at time t of day d
$\hat{P}_{train_j}(t, d)$	Production Prediction of a j-th training pattern at time t of day d
w^m	Weight of the m-th prediction model, $m = 1, \ldots, M$
σ_W^2	Source of uncertainty due to ANN model input
σ_{PR}^2	Source of uncertainty due to physical process variability
σ_{MO}^2	Source of uncertainty due to ANN model error
σ_ε^2	Overall sources of uncertainty, $\sigma_\varepsilon^2 = \sigma_W^2 + \sigma_{PR}^2 + \sigma_{MO}^2$
$\mathbf{X}_{\boldsymbol{train}}^{\boldsymbol{BS}}$	Bootstrap training dataset
$\mathbf{X}_{\boldsymbol{train}}^{\boldsymbol{MVE}}$	MVE training dataset
$RMSE$	Root Mean Square Error (in kW)
MAE	Mean Absolute Error (in kW)
$WMAE$	Weighted Mean Absolute Error
pg_{METRIC}	Prediction performance gain calculated for a performance $METRIC$
$METRIC^{Baseline}$	Prediction performance $METRIC$ obtained by a baseline prediction approach
$METRIC^{Ensemble}$	Prediction performance $METRIC$ obtained by the proposed ensemble prediction approach
Δt	Prediction horizon
$\hat{P}_{t+\Delta t}$	Prediction obtained at time t over the prediction horizon using the Smart Persistence model
P_t	True production at time t
PICP	PI Coverage Probability
PIW	PI Width (in kW)
C_{dof}^{α}	(1-α)/2 quantile of a Student t-distribution with number of degrees of freedom
PDF	Probability Density Function

ACKNOWLEDGMENT

The authors would like to acknowledge the Renewable Energy Center at the Applied Science Private University for sharing with us the Solar PV system data.

The authors would like to thank all the reviewers for their valuable comments to improve the quality of this paper.

REFERENCES

[1] G. Kosmadakis, S. Karellas, and E. Kakaras, "Renewable and conventional electricity generation systems: Technologies and diversity of energy systems," in *Renewable Energy Governance: Complexities and Challenges*, E. Michalena and J. M. Hills, Eds. London, U.K.: Springer, 2013, pp. 9–30.
[2] R. P. Varun and I. K. Bhat, "Energy, economics and environmental impacts of renewable energy systems," *Renew. Sustain. Energy Rev.*, vol. 13, no. 9, pp. 2716–2721, 2009.
[3] N. L. Panwar, S. C. Kaushik, and S. Kothari, "Role of renewable energy sources in environmental protection: A review," *Renew. Sustain. Energy Rev.*, vol. 15, no. 3, pp. 1513–1524, 2011.
[4] *Wind in Power—2016 European Statistics*, Eur. Wind Energy Assoc., Brussels, Belgium, 2017.
[5] *Renewable Energy Statistics 2018*, Int. Renew. Energy Agency, Abu Dhabi, United Arab Emirates, 2018.
[6] S. S. Reddy, "Optimization of renewable energy resources in hybrid energy systems," *J. Green Eng.*, vol. 7, nos. 1–2, pp. 43–60, 2017.
[7] *Sustainability Report 2017*, Elawan Energy S.L., Madrid, Spain, 2017.
[8] *Renewable Capacity Highlights*, Int. Renew. Energy Agency, Abu Dhabi, United Arab Emirates, 2019.
[9] *Renewable Capacity Statistics 2019*, Int. Renew. Energy Agency, Abu Dhabi, United Arab Emirates, 2019.
[10] C. Candelise, M. Winskel, and R. J. K. Gross, "The dynamics of solar PV costs and prices as a challenge for technology forecasting," *Renew. Sustain. Energy Rev.*, vol. 26, pp. 96–107, Oct. 2013.
[11] C. Kost, J. N. Mayer, J. Thomsen, N. Hartmann, C. Senkpiel, S. Philipps, S. Nold, S. Lude, N. Saad, and T. Schlegl, "Levelized cost of electricity—Renewable energy technologies," Fraunhofer Inst. Sol. Energy Syst., Freiburg, Germany, Tech. Rep. urn:nbn:de:0011-n-2799302, Nov. 2013. [Online]. Available: http://publica.fraunhofer.de/documents/N-279930.html
[12] *Renewable Power Generation Costs in 2017*, Int. Renew. Energy Agency, Abu Dhabi, United Arab Emirates, 2017.
[13] J. Antonanzas, N. Osorio, R. Escobar, R. Urraca, F. J. Martinez-de-Pison, and F. Antonanzas-Torres, "Review of photovoltaic power forecasting," *Sol. Energy*, vol. 136, pp. 78–111, Oct. 2016.
[14] R. J. Bessa, A. Trindade, C. S. P. Silva, and V. Miranda, "Probabilistic solar power forecasting in smart grids using distributed information," *Int. J. Elect. Power Energy Syst.*, vol. 72, pp. 16–23, Nov. 2015.
[15] C. B. Martinez-Anido, B. Botor, A. R. Florita, C. Draxl, S. Lu, H. F. Hamann, and B.-M. Hodge, "The value of day-ahead solar power forecasting improvement," *Sol. Energy*, vol. 129, pp. 192–203, May 2016.
[16] M. K. Behera, I. Majumder, and N. Nayak, "Solar photovoltaic power forecasting using optimized modified extreme learning machine technique," *Eng. Sci. Technol. Int. J.*, vol. 21, no. 3, pp. 428–438, 2018.
[17] S.-G. Kim, J.-Y. Jung, and K. M. Sim, "A two-step approach to solar power generation prediction based on weather data using machine learning," *Sustainability*, vol. 11, no. 5, p. 1501, 2019.
[18] S. Alessandrini, L. D. Monache, S. Sperati, and G. Cervone, "An analog ensemble for short-term probabilistic solar power forecast," *Appl. Energy*, vol. 157, pp. 95–110, Nov. 2015.
[19] S. Rosiek, J. Alonso-Montesinos, and F. J. Batlles, "Online 3-h forecasting of the power output from a BIPV system using satellite observations and ANN," *Int. J. Elect. Power Energy Syst.*, vol. 99, pp. 261–272, Jul. 2018.
[20] S. S. Reddy, "Optimal scheduling of thermal-wind-solar power system with storage," *Renew. Energy*, vol. 101, pp. 1357–1368, Feb. 2017.
[21] S. S. Reddy, V. Sandeep, and C. M. Jung, "Review of stochastic optimization methods for smart grid," *Frontiers Energy*, vol. 11, no. 2, pp. 197–209, 2017.
[22] S. S. Reddy and P. R. Bijwe, "Real time economic dispatch considering renewable energy resources," *Renew. Energy*, vol. 83, pp. 1215–1226, Nov. 2015.
[23] U. K. Das, K. S. Tey, M. Seyedmahmoudian, S. Mekhilef, M. Y. I. Idris, W. van Deventer, B. Horan, and A. Stojcevski, "Forecasting of photovoltaic power generation and model optimization: A review," *Renew. Sustain. Energy Rev.*, vol. 81, pp. 912–928, Jan. 2018.
[24] B. Espinar, J.-L. Aznarte, R. Girard, A. M. Moussa, and G. Kariniotakis, "Photovoltaic forecasting: A state of the art," in *Proc. 5th Eur. PV-Hybrid Mini-Grid Conf.*, 2010, p. 250.
[25] S. Al-Dahidi, O. Ayadi, J. Adeeb, M. Alrbai, and R. B. Qawasmeh, "Extreme learning machines for solar photovoltaic power predictions," *Energies*, vol. 11, no. 10, p. 2725, 2018.

[26] C. Monteiro, L. A. Fernandez-Jimenez, I. J. Ramirez-Rosado, A. Muñoz-Jimenez, and P. M. Lara-Santillan, "Short-term forecasting models for photovoltaic plants: Analytical versus soft-computing techniques," *Math. Problems Eng.*, vol. 2013, Oct. 2013, Art. no. 767284.

[27] E. Izgi, A. Öztopal, B. Yerli, M. K. Kaymak, and A. D. Şahin, "Short–mid-term solar power prediction by using artificial neural networks," *Sol. Energy*, vol. 86, no. 2, pp. 725–733, 2012.

[28] C. Persson, P. Bacher, T. Shiga, and H. Madsen, "Multi-site solar power forecasting using gradient boosted regression trees," *Sol. Energy*, vol. 150, pp. 423–436, Jul. 2017.

[29] H. S. Jang, K. Y. Bae, H.-S. Park, and D. K. Sung, "Solar power prediction based on satellite images and support vector machine," *IEEE Trans. Sustain. Energy*, vol. 7, no. 3, pp. 1255–1263, Jul. 2016.

[30] S. Leva, A. Dolara, F. Grimaccia, M. Mussetta, and E. Ogliari, "Analysis and validation of 24 hours ahead neural network forecasting of photovoltaic output power," *Math. Comput. Simul.*, vol. 131, pp. 88–100, Jan. 2017.

[31] A. A. Mohammed and Z. Aung, "Ensemble learning approach for probabilistic forecasting of solar power generation," *Energies*, vol. 9, no. 12, p. 1017, 2016.

[32] Y. Ren, P. N. Suganthan, and N. Srikanth, "Ensemble methods for wind and solar power forecasting—A state-of-the-art review," *Renew. Sustain. Energy Rev.*, vol. 50, pp. 82–91, Oct. 2015.

[33] M. Omar, A. Dolara, G. Magistrati, M. Mussetta, E. Ogliari, and F. Viola, "Day-ahead forecasting for photovoltaic power using artificial neural networks ensembles," in *Proc. IEEE Int. Conf. Renew. Energy Res. Appl. (ICRERA)*, Nov. 2016, pp. 1152–1157.

[34] M. Pierro, F. Bucci, M. De Felice, E. Maggioni, D. Moser, A. Perotto, F. Spada, and C. Cornaro, "Multi-Model Ensemble for day ahead prediction of photovoltaic power generation," *Sol. Energy*, vol. 134, pp. 132–146, Sep. 2016.

[35] S. Al-Dahidi, P. Baraldi, E. Zio, and M. Lorenzo, "Quantification of uncertainty of wind energy predictions," in *Proc. 3rd Int. Conf. Syst. Rel. Saf.*, 2018, pp. 1–5.

[36] K. Hornik, M. Stinchcombe, and H. White, "Multilayer feedforward networks are universal approximators," *Neural Netw.*, vol. 2, no. 5, pp. 359–366, 1989.

[37] A. Saberian, H. Hizam, M. A. M. Radzi, M. Z. A. A. Kadir, and M. Mirzaei, "Modelling and prediction of photovoltaic power output using artificial neural networks," *Int. J. Photoenergy*, vol. 2014, Apr. 2014, Art. no. 469701.

[38] M. Abuella and B. Chowdhury, "Random forest ensemble of support vector regression models for solar power forecasting," in *Proc. IEEE Power Energy Soc. Innov. Smart Grid Technol. Conf. (ISGT)*, Apr. 2017, pp. 1–5.

[39] P. P. Bonissone, F. Xue, and R. Subbu, "Fast meta-models for local fusion of multiple predictive models," *Appl. Soft Comput. J.*, vol. 11, no. 2, pp. 1529–1539, 2011.

[40] R. Polikar, "Ensemble based systems in decision making," *IEEE Circuits Syst. Mag.*, vol. 6, no. 3, pp. 21–45, Sep. 2006.

[41] L. Breiman, "Bagging predictors," *Mach. Learn.*, vol. 24, no. 2, pp. 123–140, 1996.

[42] R. E. Schapire, "The strength of weak learnability," *Mach. Learn.*, vol. 5, no. 2, pp. 197–227, 1990.

[43] Y. Freund and R. E. Schapire, "A decision-theoretic generalization of on-line learning and an application to boosting," *J. Comput. Syst. Sci.*, vol. 55, no. 1, pp. 119–139, Aug. 1997.

[44] R. Bryll, R. Gutierrez-Osuna, and F. Quek, "Attribute bagging: Improving accuracy of classifier ensembles by using random feature subsets," *Pattern Recognit.*, vol. 36, no. 6, pp. 1291–1302, 2003.

[45] M. Rigamonti, P. Baraldi, E. Zio, I. Roychoudhury, K. Goebel, and S. Poll, "Ensemble of optimized echo state networks for remaining useful life prediction," *Neurocomputing*, vol. 281, pp. 121–138, Mar. 2017.

[46] S. Al-Dahidi, F. Di Maio, P. Baraldi, and E. Zio, "A locally adaptive ensemble approach for data-driven prognostics of heterogeneous fleets," *Proc. Inst. Mech. Eng. O, J. Risk Reliab.*, vol. 231, no. 4, pp. 350–363, 2017.

[47] C. M. Bishop, *Neural Networks for Pattern Recognition*. New York, NY, USA: Oxford Univ. Press.

[48] Y. Liu, X. Yao, and T. Higuchi, "Evolutionary ensembles with negative correlation learning," *IEEE Trans. Evol. Comput.*, vol. 4, no. 4, pp. 380–387, Nov. 2000.

[49] A. Khosravi, S. Nahavandi, D. Creighton, and A. F. Atiya, "Comprehensive review of neural network-based prediction intervals and new advances," *IEEE Trans. Neural Netw.*, vol. 22, no. 9, pp. 1341–1356, Sep. 2011.

[50] Q. Ni, S. Zhuang, H. Sheng, S. Wang, and J. Xiao, "An optimized prediction intervals approach for short term PV power forecasting," *Energies*, vol. 10, no. 10, p. 1669, 2017.

[51] T. Heskes, "Practical confidence and prediction intervals," in *Proc. Adv. Neural Inf. Process. Syst.*, 1997, pp. 176–182.

[52] J. T. G. Hwang and A. A. Ding, "Prediction intervals for artificial neural networks," *J. Amer. Statist. Assoc.*, vol. 92, no. 438, pp. 748–757, Jun. 1997.

[53] D. A. Nix and A. S. Weigend, "Estimating the mean and variance of the target probability distribution," in *Proc. IEEE Int. Conf. Neural Netw.*, vol. 1, Jul. 1994, pp. 55–60.

[54] A. Khosravi, S. Nahavandi, D. Creighton, and A. F. Atiya, "Lower upper bound estimation method for construction of neural network-based prediction intervals," *IEEE Trans. Neural Netw.*, vol. 22, no. 3, pp. 337–346, Dec. 2011.

[55] S. L. Ho, M. Xie, L. C. Tang, K. Xu, and T. N. Goh, "Neural network modeling with confidence bounds: A case study on the solder paste deposition process," *IEEE Trans. Electron. Packag. Manuf.*, vol. 24, no. 4, pp. 323–332, Oct. 2001.

[56] *Predicting Solar Power Production: Irradiance Forecasting Models, Applications and Future Prospects*, Sol. Electr. Power Alliance, Washington, DC, USA, 2014.

[57] S. Al-Dahidi, P. Baraldi, E. Zio, and E. Legnani, "A dynamic weighting ensemble approach for wind energy production prediction," in *Proc. 2nd Int. Conf. Syst. Rel. Saf. (ICSRS)*, Dec. 2018, pp. 296–302.

[58] Applied Science Private University. *PV System ASU09: Faculty of Engineering*. Accessed: Feb. 17, 2019. [Online]. Available: http://energy.asu.edu.jo/

[59] C. J. Schwarz, "Sampling, regression, experimental design and analysis for environmental scientists, biologists, and resource managers," Dept. Statist. Actuarial Sci., Simon Fraser Univ., Burnaby, BC, Canada, Course Notes, 2011.

[60] Z. I. Botev, J. F. Grotowski, and D. P. Kroese, "Kernel density estimation via diffusion," *Ann. Stat.*, vol. 38, no. 5, pp. 2916–2957, 2010.

[61] Google Maps. (2018). *Applied Science*. Private University. Accessed: Nov. 20, 2018. [Online]. Available: https://goo.gl/qA4h3w

[62] M. H. Alomari, O. Younis, and S. M. A. Hayajneh, "A predictive model for solar photovoltaic power using the Levenberg-Marquardt and Bayesian regularization algorithms and real-time weather data," *J. Adv. Comput. Sci. Appl.*, vol. 9, no. 1, pp. 347–353, 2018.

[63] M. Paulescu, M. Brabec, R. Boata, and V. Badescu, "Structured, physically inspired (gray box) models versus black box modeling for forecasting the output power of photovoltaic plants," *Energy*, vol. 121, pp. 792–802, Feb. 2017.

[64] T.-C. Yu and H.-T. Chang, "The forecast of the electrical energy generated by photovoltaic systems using neural network method," in *Proc. Int. Conf. Electr. Inf. Control Eng.*, Apr. 2011, pp. 2758–2761.

[65] C. Schwingshackl, M. Petitta, J. E. Wagner, G. Belluardo, D. Moser, M. Castelli, M. Zebisch, and A. Tetzlaff, "Wind effect on PV module temperature: Analysis of different techniques for an accurate estimation," *Energy Procedia*, vol. 40, pp. 77–86, Jan. 2013.

[66] M. H. Alomari, J. Adeeb, and O. Younis, "Solar photovoltaic power forecasting in jordan using artificial neural networks," *Int. J. Elect. Comput. Eng.*, vol. 8, no. 1, p. 497, 2018.

[67] K. U. Das, S. K. Tey, M. Seyedmahmoudian, Y. M. Idna Idris, S. Mekhilef, B. Horan, and A. Stojcevski, "SVR-based model to forecast PV power generation under different weather conditions," *Energies*, vol. 10, no. 7, p. 876, 2017.

[68] M. Malvoni, M. G. De Giorgi, and P. M. Congedo, "Data on support vector machines (SVM) model to forecast photovoltaic power," *Data Brief*, vol. 9, pp. 13–16, Dec. 2016.

[69] B. Wolff, E. Lorenz, and O. Kramer, "Statistical learning for short-term photovoltaic power predictions," in *Computational Sustainability* (Studies in Computational Intelligence), vol. 645. Cham, Switzerland: Springer, 2016, pp. 31–45. doi: 10.1007/978-3-319-31858-5_3.

[70] T. Hastie, R. Tibshirani, and J. H. Friedman, *The Elements of. Statistical Learning: Data Mining, Inference, and Prediction*. New York, NY, USA: Springer-Verlag, 2001.

[71] R. M. Ehsan, S. P. Simon, and P. R. Venkateswaran, "Day-ahead forecasting of solar photovoltaic output power using multilayer perceptron," *Neural Comput. Appl.*, vol. 28, no. 12, pp. 3981–3992, 2017.

[72] Z. Li, M. S. M. Rahman, R. Vega, and B. Dong, "A hierarchical approach using machine learning methods in solar photovoltaic energy production forecasting," *Energies*, vol. 9, no. 1, p. 55, 2016.

[73] S. Lawrence, C. L. Giles, and A. C. Tsoi, "What size neural network gives optimal generalization? Convergence properties of backpropagation," Dept. Comput. Sci., Univ. Maryland, College Park, MD, USA, Tech. Rep. UMIACS-TR-96-22 CS-TR-3617, 1996, pp. 1–37.

[74] P. J. Braspenning, F. Thuijsman, and A. J. M. M. Weijters, *Artificial Neural Networks: An Introduction to ANN Theory and Practice*, vol. 931. Berlin, Germany: Springer-Verlag, 1995.
[75] P. Baraldi, F. Mangili, and E. Zio, "Ensemble of bootstrapped models for the prediction of the remaining useful life of a creeping turbine blade," in *Proc. IEEE Conf. Prognostics Health Manage. (PHM)*, Jun. 2012, pp. 1–8.
[76] Y. K. Semero, J. Zhang, and D. Zheng, "PV power forecasting using an integrated GA-PSO-ANFIS approach and Gaussian process regression based feature selection strategy," *CSEE J. Power Energy Syst.*, vol. 4, no. 2, pp. 210–218, 2018.
[77] J. Kennedy, "Particle swarm optimization," in *Encyclopedia of Machine Learning*, C. Sammut and G. I. Webb, Eds. Boston, MA, USA: Springer, 2011.
[78] X.-S. Yang and S. Deb, "Cuckoo search via Lévy flights," in *Proc. World Congr. Nature Biol. Inspired Comput. (NaBIC)*, Dec. 2009, pp. 210–214.
[79] E. Ogliari, A. Niccolai, S. Leva, and R. E. Zich, "Computational intelligence techniques applied to the day ahead PV output power forecast: Phann, sno and mixed," *Energies*, vol. 11, no. 6, p. 1487, 2018.
[80] K. Orwig, C. Clark, J. Cline, S. Benjamin, J. Wilczak, M. Marquis, C. Finley, A. Stern, and J. Freedman, "Enhanced short-term wind power forecasting and value to grid operations," in *Proc. 11th Annu. Int. Large-Scale Integr. Wind Power Syst.*, 2012.
[81] K. Orwig, C. Clark, J. Cline, S. Benjamin, J. Wilczak, M. Marquis, C. Finley, A. Stern, and J. Freedman, "Economic evaluation of short-term wind power forecasts in ERCOT: Preliminary results," in *Proc. 11th Int. Workshop Large-Scale Integr. Wind Power Power Syst. Transmiss. Netw. Offshore Wind Power Plants*, Lisbon, Portugal, Nov. 2012. [Online]. Available: http://windintegrationworkshop.org/wp-content/uploads/sites/18/2016/02/WIW12_Proceedings_Content_Overview.pdf
[82] M. C. Moura, I. D. Lins, R. J. Ferreira, E. L. Droguett, and C. M. C. Jacinto, "Predictive maintenance policy for oil equipment in case of scaling through support vector machines," in *Proc. Adv. Saf., Rel. Risk Manage. (ESREL)*, 2011, pp. 503–507.
[83] L. Jaulin, *Applied Interval Analysis: With Examples in Parameter and State Estimation, Robust Control and Robotics*. London, U.K.: Springer, 2001. doi: 10.1007/978-1-4471-0249-6.
[84] R. Dybowski and S. Roberts, "Confidence intervals and prediction intervals for feedforward neural networks," in *Clinical Applications of Artificial Neural Networks*, R. Dybowski and V. Gant, Eds. Cambridge, U.K.: Cambridge Univ. Press, 2001, pp. 298–326. doi: 10.1017/CBO9780511543494.013.

SAMEER AL-DAHIDI was born in Kuwait, in 1986. He received the B.Sc. degree (with honors) in electrical engineering from The Hashemite University, Zarqa, Jordan, in 2008, the M.Sc. degree in nuclear energy (operations specialty) from Ecole Centrale Paris and Université Paris-Sud 11, Paris, France, in 2012, and the Ph.D. degree (with honors) in energetic and nuclear science and technology from Politecnico di Milano, Milan, Italy, in 2016.

He is currently an Assistant Professor with the Mechanical and Maintenance Engineering Department, School of Applied Technical Sciences, the German Jordanian University, Amman, Jordan, since February 2018. His current research interests include the development of analytics and models for Prognostics and Health Management (PHM), operation, maintenance and reliability, availability, maintainability, and safety (RAMS) analysis of engineering systems, and the development of artificial intelligence (AI)-based methods for renewable energy production prediction. In addition, he has interests in renewable energy systems and mechanical engineering fields such as thermal sciences, heating, ventilation and air-conditioning (HVAC), and others. He has published several articles in high quality journals, such as *Applied Soft Computing, Expert Systems with Applications, Advances in Mechanical Engineering, International Journal of Prognostics and Health Management, Reliability Engineering and System Safety, Energies, and Entropy.*

OSAMA AYADI received the B.Sc. degree and was ranked first in mechanical engineering from the University of Jordan, the M.Sc. degree in mechanical engineering-solar energy from Dalarna University in Sweden, and the Ph.D. degree in energy from Politecnico di Milano, Italy. He was an active member in the International Energy Agency tasks 38 (solar air-conditioning and refrigeration) and Task 44 (solar and heat pump systems). He is also a member of the International Solar Energy Society (ISES). He is currently an Assistant Professor with the Mechanical Engineering Department, University of Jordan. He is involved in the development of several postgraduate and undergraduate programs and courses in the fields of sustainability, environment, and energy such as: MUREE, MANSUR, CLIMASP, and EGREEN.

MOHAMMED ALRBAI received the B.Sc. degree and was ranked first in mechanical engineering from Hashemite University, the M.Sc. degree in mechanical engineering from the Jordan University of Science and Technology, Jordan, and the Ph.D. degree in combustion and thermal science from West Virginia University, USA. He is currently an Assistant Professor with the Mechanical Engineering Department, University of Jordan. He is involved in the development of several postgraduate and undergraduate programs and courses in the fields of sustainability, environment, and energy such as: EGREEN, SEMSEM, and HEBA.

JIHAD ADEEB received the B.Sc. degree in mechanical engineering from the Faculty of Engineering Technology, Al-Balqa Applied University, Amman, Jordan, in 2015. He is currently pursuing the M.Sc. degree in renewable energy engineering from The University of Jordan, Amman, Jordan. He is currently a Solar System Engineer in a private company in Saudi Arabia. His research interests include PV panels technologies and machine learning applications in renewable energy.